Industrial Lubrication and Tribology

Study on thermo-mechanical coupling characteristics of angle contact ball bearing with fix-position preload

Pingping He, Feng Gao, Yan Li, Wenwu Wu, Dongya Zhang,

Study on thermo-mechanical coupling characteristics of angle contact ball bearing with fix-position preload

Pingping He
Key Laboratory of NC Machine Tools and Integrated Manufacturing Equipment of the Education Ministry and Key Laboratory of Manufacturing Equipment of Shaanxi Province, Xi'an University of Technology, Xi'an, China and Mechanic and Electronic Engineering of Sanmenxia Polytechnic, Sanmenxia, China, and

Feng Gao, Yan Li, Wenwu Wu and Dongya Zhang
Key Laboratory of NC Machine Tools and Integrated Manufacturing Equipment of the Education Ministry and Key Laboratory of Manufacturing Equipment of Shaanxi Province, Xi'an University of Technology, Xi'an, China

Abstract

Purpose – Under fix-position preload, the high rotation speed of the angular contact ball bearing exacerbates the frictional heat generation, which causes the increase of the bearing temperature and the thermal expansion. The high rotation speed also leads to the centrifugal expansion of the bearing. Under the thermal and centrifugal effect, the structural parameters of the bearing change, affecting the mechanical properties of the bearing. The mechanical properties of the bearing determine its heat generation mechanism and thermal boundary conditions. The purpose of this paper is to study the effect of centrifugal and thermal effects on the thermo-mechanical characteristics of an angular contact ball bearing with fix-position preload.

Design/methodology/approach – Because of operating conditions, elastic deformation occurs between the ball and the raceway. Assuming that the surfaces of the ball and channel are absolutely smooth and the material is isotropic, quasi-static theory and thermal network method are used to establish the thermo-mechanical coupling model of the bearing, which is solved by Newton–Raphson iterative method.

Findings – The higher the rotation speed, the greater the influence of centrifugal and thermal effects on the bearing dynamic parameters, temperature rise and actual axial force. The calculation results show that the effects of thermal field on bearing dynamic parameters are more significant than the centrifugal effect. The temperature rise and actual axial force of the bearing are measured. Comparing the calculation and the experimental results, it is found that the temperature rise and the actual axial force of the bearing are closer to reality considering thermal and centrifugal effects.

Originality/value – In the past studies, the thermo-mechanical coupling characteristics research and experimental verification of angular contact ball bearing with fix-position preload are not concerned. Research findings of this paper provide theoretical guidance for spindle design.

Keywords Newton–Raphson method, Thermal-mechanical coupling, Centrifugal and thermal expansion, Fix-position preload

Paper type Research paper

Nomenclature

- A^0 = distance between centers of curvature of inner and outer race groove under initial conditions (mm);
- A^2 = distance between centers of curvature of inner and outer race groove under assembly stress and initial preload (mm);
- A = contact ellipse area;
- a = semi-major width of contact area (mm);
- b = semi-minor width of contact area (mm);
- B = inner ring width (mm);
- C = outer ring width (mm);
- C_p = Specific heat (J/kg·K);
- D_h = housing outer diameter (mm);
- D = bearing outer diameter (mm);
- d = bearing inner diameter (mm);
- d_b = ball diameter (mm);
- d_i = inside diameter (mm);
- d_m = pitch diameter (mm);
- d_o = outside diameter (mm);
- d_2 = the inner diameter of the shaft (mm);
- E = Young's modulus (GPa);
- F_{cj} = centrifugal force (N);
- f = groove curvature coefficient;
- h = heat transfer coefficient W/(mm^2·K);
- H = the frictional heat generation (W);
- k = thermal conductivity W/(mm·K);

The current issue and full text archive of this journal is available on Emerald Insight at: **www.emeraldinsight.com/0036-8792.htm**

Industrial Lubrication and Tribology
© Emerald Publishing Limited [ISSN 0036-8792]
[DOI 10.1108/ILT-10-2018-0390]

The research is financially supported by the National Natural Science Foundation of China (51775432) and the Key R & D projects in Shaanxi (2018ZDXM-GY-074).

Received 6 November 2018
Revised 19 December 2018
Accepted 12 January 2019

K_n = load-deflection parameter ($N/mm^{1.5}$);
L_h = initial center lengths (mm);
M_{isj} = the spin friction torque (N·m);
n = rotation speed (r/min);
M_v = lubrication drag friction torque (N·m);
$Q_{i(o)j}$ = the contact load between the *j*th ball and the inner (outer) raceway (N);
R = thermal resistance (W/K);
T = node temperature (°C);
ΔT = the temperature rise (°C);
T_a = air temperature (°C);
Z = balls number;
$T_{i(o)j}$ = the friction between the *j*th ball and the inner (outer) raceway (N);
$V_{i(o)yj}$ = the sliding speed along the major axis of the contact ellipse in the inner(outer) sliding contact region (m/s);
ν_g = the kinematic viscosity of grease (mm^2/s);
α^0 = initial contact angle (°);
α_b = thermal expansion coefficient of the ball;
α = contact angle under assembly stress and initial preload (°);
$\alpha_{i(o)j}$ = contact angle between the *j*th ball and the inner (outer) raceway under operating conditions (°);
β_j = pitch angle (°);
ω = angular velocity of the spindle (rad/s);
ω_{isj} = spin angular velocity (rad/s);
ω_i = angular velocity of the inner ring (rad/s);
ω_b = angular velocity of the ball (rad/s);
ρ = density (kg/m^3);
μ = friction coefficient;
ξ_b = Poisson ratio of the bearing;
ξ_s = Poisson ratio of the spindle;
Γ = Second type elliptic integral;
$\tau_{i(o)yj}$ = tangential stress along the major axis of the contact ellipse in the inner(outer) sliding contact region (MPa); and
$\delta_{i(o)j}$ = contact deformation between the *j*th ball and the inner(outer) raceway under (mm).

Subscripts

j = the *j*th ball;
i = inner ring;
o = outer ring;
b = ball;
h = housing;
s = spindle;
g = grease; and
1, 2,...7 = node number.

Superscripts

0 = initial; and
1 = interference fit.

1. Introduction

Angular contact ball bearings are widely used in machine tools because of their high reliability and low power consumption (Hwang and Lee, 2010; Wang and Wang, 2015; Cao *et al.*, 2017). When the spindle runs at high speed, a great amount of heat will be produced in the bearing, which will lead to the thermal deformation of the spindle and will reduce the motion accuracy of the spindle. The thermal characteristics of the bearing will significantly change its mechanical properties. However, thermal boundary conditions are determined by the mechanical properties. Therefore, it is important and urgent to establish an accurate thermo-mechanical coupling model of the bearing.

Jones (1959) first studied the motion and a partial sliding friction of the angular contact ball bearing by quasi-static analysis method. Palmgren (1959) summered the empirical formula of friction torque for rolling bearings through a large number of experiments on various types and sizes of bearings. Harris (1971) deduced the calculation method of frictional power consumption in different parts of rolling bearings to estimate the heat generation of the bearing. Harris (1991) analyzed the temperature distribution of bearing system with the heat network method. Bossmanns and Tu (1999) referred to Harris's research results on the heating mechanism of ball bearings. A qualitative power flow model is proposed to describe the temperature field distribution of high-speed motorized spindle (Bossmanns and Tu, 2001). Jiang *et al* (2000) put forward a method for calculating the internal heat generation of the rolling bearing with spin friction torque. The above studies mainly focus on the heat generation model and temperature field distribution of the bearing, the thermo-mechanical coupling effect of the bearing is not considered in the calculation process.

The finite element method is used by Lin *et al.* (2003) to solve the thermo-mechanical coupling equation of the spindle. Li and Shin (2004) developed a comprehensive thermo-mechanical model for predicting the thermal and dynamic responses of spindle systems based on the finite element method. The finite element analysis model of the motorized spindle was established by Xiao *et al.* (2008) based on thermal-structural coupling. Holkup (2010) presented a calculation model to predict the influence of the temperature distribution in the spindle system. Taking into account the centrifugal effect of the spindle, the gyro torque and the softening effect of the bearing stiffness, Tian *et al.* (2008) designed a thermo-mechanical coupling model of the spindle-bearing system. Hu *et al.* (2014) proposed a thermo-mechanical coupling analysis method of angular contact ball bearings utilizing multi-software collaborative computing platform. The thermo- mechanical model of the high speed spindle is established by Zivkovic (2015) to determine the change of the static stiffness of the spindle and the effect of the thermal expansion on the machining precision according to the prediction of the bearing characteristics. The transient thermal analysis equation on the basis of the steady state network method was deduced by Yan and Hong (2016). Than and Huang (2016) predicted nonlinear thermal characteristics of a high-speed spindle bearing in according with a quasi-static model and finite difference method. The above researches mainly focus on the thermo-mechanical coupling model of the spindle. At present, front bearings of most spindles are greased and fix-position preloaded. A comparison model is built to analyze the stiffness of angular contact ball bearings under different preload mechanisms by Zhang *et al.* (2017a, 2017b). However, the theoretical research and experimental verification of the thermo-mechanical characteristics of the bearing with grease lubrication and fix-position preload are rarely reported.

In this paper, the deformation of the bearing caused by centrifugal and thermal expansion is considered. Based on quasi-static theory and thermal network method, the thermo-mechanical coupling model of angular contact ball bearing with grease lubrication and fix-position preload is established. The Newton–Raphson method is used to solve this model.

2. Thermo-mechanical coupling model

Assuming that the surfaces of the ball and channel are absolutely smooth, the material is isotropic, and elastic deformation occurs between the ball and the raceway, the thermo-mechanical coupling model of the bearing will be established.

2.1 Deformation of angle contact ball bearing under static load

Interference fit is used usually when bearing inner ring and rotation shaft are installed. The variation of curvature center of inner and outer raceways and bearing contact angle under the action of assembly stress and initial preload is shown in Figure 1. The radial displacement u_i of the inner ring caused by interference fit I can be expressed as (Zhang *et al.*, 2017a, 2017b):

$$u_i = \frac{I\left(\frac{d_i}{d}\right)}{\left[\left(\frac{d_i}{d}\right)^2 - 1\right]\left\{\left[\frac{\left(\frac{d_i}{d}\right)^2+1}{\left(\frac{d_i}{d}\right)^2-1} + \xi_b\right] + \frac{E_b}{E_s}\left[\frac{\left(\frac{d}{d_2}\right)^2+1}{\left(\frac{d}{d_2}\right)^2-1} + \xi_s\right]\right\}} \tag{1}$$

According to the geometric relationship between the center of curvature of the inner and the outer groove, the contact angle α^1 under assembly stress is:

$$\alpha^1 = \mathrm{atan}\left(\frac{A sin\alpha^0}{A\cos\alpha + u_c}\right) \tag{2}$$

The distance A^1 between centers of curvature of inner and outer race groove under assembly stress is:

Figure 1 Schematic diagram of bearing under initial preload and assembly stress

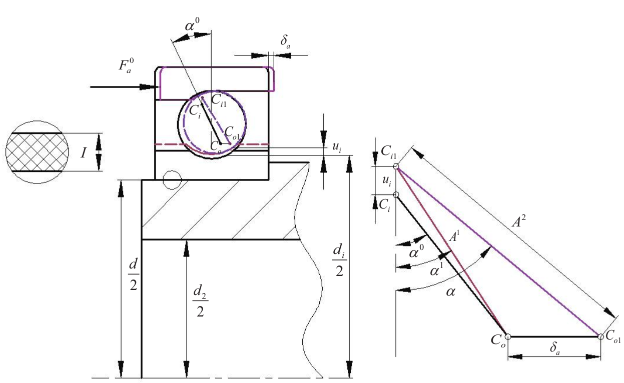

$$A^1 = A^0 sin\alpha^0 / sin\alpha^1 \tag{3}$$

Here, $A^0 = (f_i + f_o - 1)d_b$.
Under initial preload $F_a{}^0$, the curvature center of outer ring groove moves from C_o to C_{o1}, The relationship between the contact angles α^1 and α is as follows (Harris and Kotzalas, 2006):

$$\frac{F_a^0}{ZK_n(A^1)^{1.5}} = \sin\alpha\left(\frac{\cos\alpha^1}{\cos\alpha} - 1\right)^{1.5} \tag{4}$$

Here, K_n represents the Hertz contact stiffness.

The equation (4) is solved numerically using the Newton–Raphson iterative method, the actual contact angle α under the initial preload can be obtained.

Therefore, the axial displacement δ_a of the outer ring under static state is:

$$\delta_a = A^1(\cos\alpha^1\tan\alpha - \sin\alpha^1) \tag{5}$$

2.2 Thermo-mechanical coupling model of angular contact ball bearing

The centrifugal expansion of the inner ring is caused by the inertia load at high speed. According to the elastic theory of Timoshenko beam, the expression δ_c of the radial displacement of the inner ring at d_i is (Harris and Kotzalas, 2006):

$$\delta_c = \delta_{r=\frac{d_i}{2}} = C_1\frac{d_i}{2} + \frac{C_2}{\left(\frac{d_i}{2}\right)} - \frac{1-\xi_s^2}{8E}\rho\omega^2\left(\frac{d_i}{2}\right)^3 \tag{6}$$

Here, C_1, C_2 are constants.

Under the operating conditions, the thermal expansion is because of the bearing heat generated, as shown in Figure 2. Its corresponding thermal expansion model is referred to the work of (Lin *et al.*, 2003).

When the bearing temperature increases, the expansion difference δ_r of inner ring and outer ring in the radial direction is:

$$\delta_r = 0.5\alpha_s(d_i\Delta T_i - d_o\Delta T_o) \tag{7}$$

The thermal expansion δ_b of the ball can be expressed as:

Figure 2 Thermal deformations of the bearing

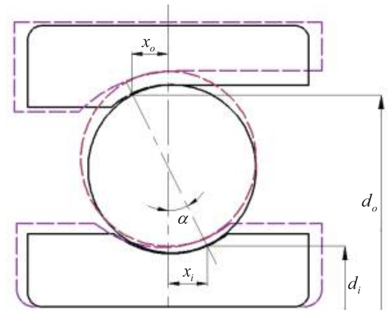

$$\delta_b = \alpha_b d_b \Delta T_b \tag{8}$$

It is assumed that the curvature center position of bearing outer raceway is unchanged, the center position of the ball and the displacement of the curvature center of the inner raceway is further changed because of the centrifugal and thermal effect as shown in Figure 3.

The geometric equation of the raceway curvature center and the center of the ball is:

$$\begin{cases} A_{1j} = l_{oj}sin\alpha_{oj} + l_{ij}\sin\alpha_{ij} \\ A_{2j} = l_{oj}\cos\alpha_{oj} + l_{ij}\cos\alpha_{ij} \end{cases} \tag{9}$$

Here, $l_{ij} = (f_i - 0.5)d_b + \delta_{ij}$, $l_{oj} = (f_o - 0.5)d_b + \delta_{oj}$.

Under the combined action of centrifugal load, thermal load and preload, the geometric relationship between the curvature center of the raceway and the center of the ball is:

$$\begin{cases} A_{1j} = A\sin\alpha + \delta_a \\ A_{2j} = Acos\alpha + \delta_r + \delta_c \end{cases} \tag{10}$$

The force of analysis the ball is shown in Figure 4. The equilibrium equation for each ball j (j = 1, ..., Z) can be established as follows:

$$\begin{cases} Q_{ij}\cos\alpha_{ij} - Q_{oj}\cos\alpha_{oj} - T_{ij}\sin\alpha_{ij} + T_{oj}\sin\alpha_{oj} + F_{cj} = 0 \\ Q_{ij}\sin\alpha_{ij} - Q_{oj}\sin\alpha_{oj} + T_{ij}\cos\alpha_{ij} - T_{oj}\cos\alpha_{oj} = 0 \end{cases} \tag{11}$$

Above parameters are explained in detail (Zhang *et al.*, 2017a, 2017b).

Under the fix-position preload, the actual axial load of the bearing can be written as:

Figure 3 Position of the center of the curvature before and after centrifugal and thermal expansion

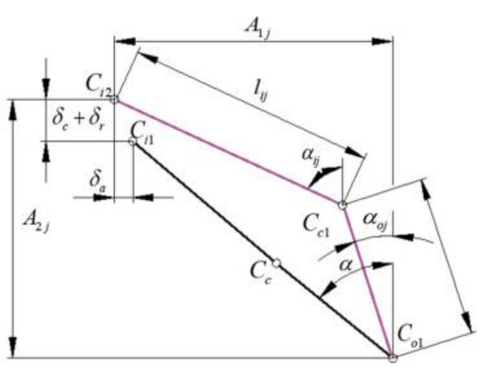

Figure 4 The force diagram on the rolling element

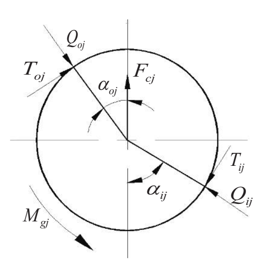

$$F_a = \sum_{j=1}^{z}(Q_{oj}\sin\alpha_{oj}) \tag{12}$$

2.3 Heat generation

The heat generated in the bearing mainly derived from the friction between the ball and the raceway. For grease lubricated angular contact ball bearing, the frictional heat mainly includes the heat generated by the differential sliding of the contact area between the ball and the raceway, the heat by spin sliding of the ball, the heat by the lubrication drag friction, the heat by the gyroscopic motion, and the heat by sliding between the ball and the cage. In engineering practice, the gyroscopic motion is almost negligible because of the preload force. The heat resulted from sliding between the ball and the cage is minimal and can be ignored for most of the time (Wang, 2013).

2.3.1 Differential sliding friction between the ball and the raceway

Surface contact between ball and raceway will cause differential slip between these two surfaces. Under the action of the slip speed and friction, the frictional heat generation $H_{1i(o)yj}$ along the short axis of the contact ellipse in the inner(outer) contact sliding regions of the jth ball is expressed as (Wang, 2013):

$$H_{1i(o)yj} = \iint_{\Omega} \tau_{i(o)yj} V_{i(o)yj} dA, \Omega : \left(\frac{x}{a_{i(o)j}}\right)^2 + \left(\frac{y}{b_{i(o)j}}\right)^2 = 1 \tag{13}$$

2.3.2 Ball spin friction heat generation

Spin friction is another source of bearing heat generation. According to the assumption of raceway control, the ball and the outer ring have pure rolling without spin motion. The spin friction heat generation H_{2ij} of the jth ball is expressed as (Zivkovic, 2015):

$$H_{2ij} = M_{isj}\omega_{isj} \tag{14}$$

Here, $M_{isj} = \frac{3\mu Q_{ij} a_{ij} \Gamma}{8}$,

$$\omega_{isj} = \left(-\frac{\omega_b}{\omega_i}\cos\beta_j\sin\alpha_{ij} + \frac{\omega_b}{\omega_i}\sin\beta_j\cos\alpha_{ij} + \sin\alpha_{ij}\right)\omega_i$$

2.3.3 Lubricating and dragging friction heat

Because of the viscosity drag generated by the viscosity of the grease, the heat generation is (Than and Huang, 2016):

$$H_3 = M_\nu \omega_r \tag{15}$$

Here,

$$M_\nu = \begin{cases} 10^{-7} f_0 (\upsilon_g n)^{2/3} d_m^3 & \upsilon_g n \geq 2000 \\ 160 \times 10^7 f_0 d_m^3 & \upsilon_g n < 2000 \end{cases},$$

$$\omega_r = \omega d_m / d_b$$

The frictional heat of inner and outer raceway of the bearing can be expressed as:

$$H_i = \sum_{j=1}^{Z} H_{1iyj} + \sum_{j=1}^{Z} H_{2ij} + \frac{H_3}{2} \tag{16}$$

$$H_o = \sum_{j=1}^{Z} H_{1oyj} + \frac{H_3}{2} \tag{17}$$

2.4 Thermal network model

In this paper, the thermal network method is used to analyze the temperature field of the bearing, and the thermal nodes are arranged in the bearing, and connected to form a thermal network with different forms of thermal resistance. The bearing seven-node model (Yan and Hong, 2016) is shown in Figure 5.

Based on the Kirchhoff's law of electricity, the heat network diagram is used, which ignores the influence of the lubricating grease convection, the heat balance equations of each node of the grease lubricated bearing system are set up as equation (17).

$$\begin{cases} \dfrac{T_0 - T_1}{R_{s-s0}} + \dfrac{T_0 - T_a}{R_{s0-a}} = 0 \\ \dfrac{T_1 - T_0}{R_{s-s0}} + \dfrac{T_1 - T_2}{R_{i-s}} = 0 \\ \dfrac{T_2 - T_1}{R_{i-s}} + \dfrac{T_2 - T_4}{R_{i-g}} = H_i \\ \dfrac{T_4 - T_2}{R_{i-g}} + \dfrac{T_4 - T_3}{R_{b-g}} = 0 \\ \dfrac{T_4 - T_3}{R_{b-g}} + \dfrac{T_4 - T_5}{R_{g-o}} = 0 \\ \dfrac{T_5 - T_4}{R_{g-o}} + \dfrac{T_5 - T_6}{R_{o-h}} = H_o \\ \dfrac{T_6 - T_5}{R_{o-h}} + \dfrac{T_6 - T_7}{R_{h-h7}} = 0 \\ \dfrac{T_7 - T_6}{R_{h-h7}} + \dfrac{T_7 - T_a}{R_{h7-a}} = 0 \end{cases} \tag{18}$$

Here, the calculation of R_{i-s}, R_{i-g}, R_{i-g}, R_{b-g}, $R_{o\text{-}g}$ and R_{o-h} are detailed in the literature (Yan and Hong, 2016):

$$R_{h-h7} = \frac{Z\ln\left(\frac{D_h}{D}\right)}{2k_h \pi C}, R_{h7-a} = \frac{Z}{2h_h \pi D_h L_h},$$

Figure 5 Bearing system nodes distribution

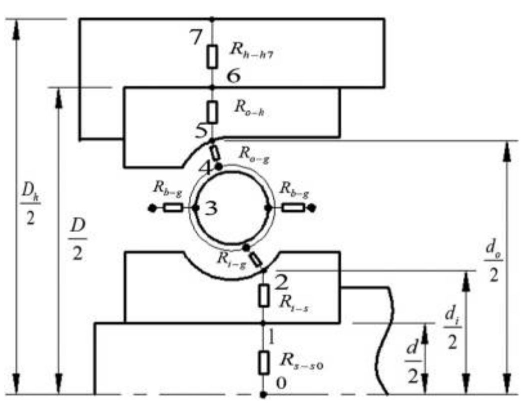

Figure 6 Flow chart for solving thermo-mechanical model

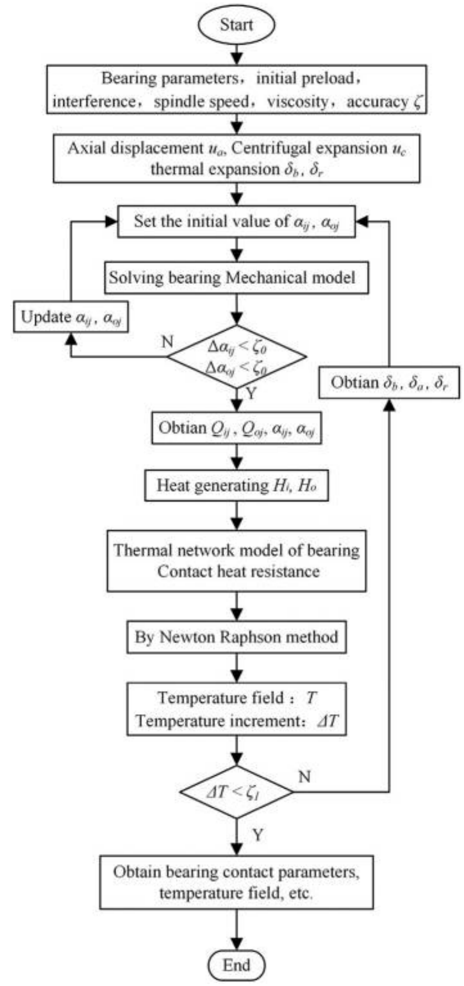

Figure 7 The testing bearing system

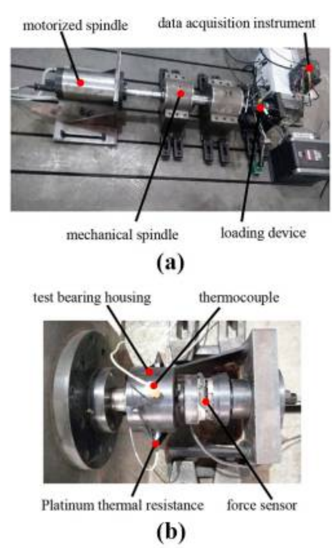

Notes: (a) Test platform; (b) sensor arrangement

Table I Parameters of the bearing system

Parameter	Figure
B	15 mm
C	15 mm
D	40 mm
d_b	7.5 mm
d_m	53.6 mm
d_o	57.3 mm
d_i	50.6 mm
D	68 mm
D_h	120 mm
f_i	0.52
f_o	0.52
Z	19
E	206 GP a
ρ	7,810 kg/m^3
α^0	15°
ξ_b	0.3

Figure 8 Radial deformation under rotation speed

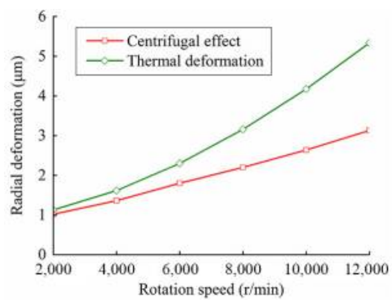

Figure 9 Dynamic parameters under different speeds

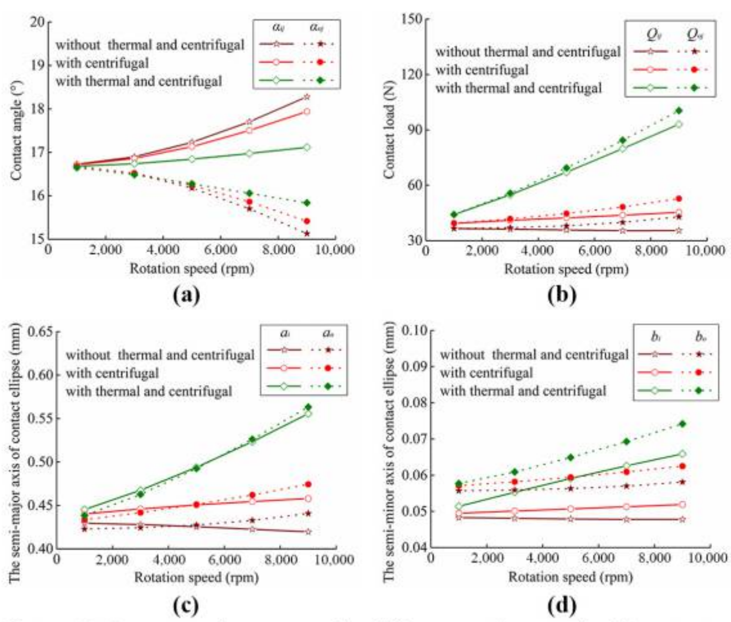

Notes: (a) Contact angle curves under different rotation speeds; (b) contact load curves under different rotation speeds; (c) the semi-major axis of contact ellipse curves; (d) the semi-minor axis of contact ellipse curves

$$R_{s-s0} = \frac{2Z}{k_s \pi B}, R_{s0-a} = \frac{4ZL_s}{k_s \pi d^2} + \frac{4Z}{h_s \pi d^2}$$

The calculation process of thermo-mechanical coupling model of the bearing is shown in Figure 6.

3. Experiment and discussion

3.1 Experimental equipment

The test platform is shown in Figure 7(a). FAG B7008C bearing and special grease(NLGI:2-3, working temperature range: $-40\sim120$°C, the viscosity of base oil at 40°C is 25 mm^2/s) are used, the initial interference fit between the shaft and the inner ring is 5 μm, and the structural and material parameters of the bearing system are shown in Table I.

During the testing process, the sensor layout is shown in Figure 7(b). A three-component force sensor TR3D-A-1K is used to monitor actual axial load of the bearing. Three platinum thermal resistors PT100 are mounted in the holes which are uniform distributed in the circumferential direction of the bearing housing surface matched with the outer ring. The thermocouple is attached to the surface of the bearing housing, and is in a circumference with the platinum thermal resistors. The sensors' data are obtained by multi-channel data logger HIOKI.

3.2 Results and discussion

3.2.1 Bearing deformation and dynamic parameters curves.

The initial preload of the bearing is 200 N. According to the flow chart in Figure 6, the radial displacement of the inner ring considering the centrifugal effect or the thermal effect is calculated by a MATLAB program. The radial deformation of the inner ring at different rotation speeds is shown in Figure 8.

About these two effects, the thermal effect contributes the most deformation of the inner ring.

The effects of thermal and centrifugal effects on the contact angle, contact load and other parameters of the bearing at different rotation speeds are calculated as shown in Figure 9 (a)-(d). It can be seen from Figure 9 that as the rotation speed increases, the internal contact angle rises up and the external contact angle decreases gradually. At 9,000 rpm, compared to contact status without considering the thermal and the centrifugal effect, the internal contact angle reduces by 1.5°, the external contact angle increased with 0.8°, and the internal and external contact loads increased to 107.9 and 118.5 per cent, respectively, when both of them are considered. When the centrifugal and the thermal effect are not considered, the internal contact load gradually decreases with the increase of the speed, and the external contact load increases. The trend of the elliptical contact semi-major(minor) axis is similar to the inner(outer) contact load. As compared to the centrifugal effect, the thermal effect has a greater impact on dynamic parameters.

Table II Temperature rise of bearing nodes

	Temperature rise (°C)			
Node no.	**3,000 rpm**	**5,000 rpm**	**7,000 rpm**	**9,000 rpm**
1	5.3	7.9	11.1	16.7
2	6.3	9.1	12.5	18.2
3	5.8	8.5	11.6	17
4	6.1	8.8	12	17.5
5	6	8.6	11.7	17.2
6	5.7	8.2	11.3	16.6
7	5.3	7.7	10.7	15.8

3.2.2 Bearing temperature rise and actual axial force curves

Calculation results with bearing heat network model are shown in Table II applied by an initial preload of 200 N, ambient temperature 24°C and the rotational speed range from 3,000 to 9,000 rpm. To verify the model proposed in this paper, the temperature rise of the outer ring of the experimental bearing and the actual preload of the bearing are measured under the same condition as the calculation, as shown in Figure 10 (a) and (b).

The temperature rise and the actual axial load obtained the experiment, the proposed method and Harris' (1971) method are compared as shown in Figure 10 (c) and (d), respectively. It can be seen that at 9,000 rpm, the temperature rise obtained the proposed method and Harris's method is 16.8°C and 11.2°C, respectively, the actual axial load is 432.9 N and 213 N, respectively. It can be found the temperature rise and the actual axial load obtained the proposed method considering centrifugal and thermal effects match the experiment well. As compared with the calculation results, the maximum error obtained the proposed method of temperature rise and actual axial load is 12.56 and 8.3 per cent, respectively.

The thermal deformation of the bearing causes a significant change in the actual axial load, makes the bearing to further generate heat and thermal deformation. The higher the rotation speed, the more significant the temperature rise of the bearing, the greater the actual axial load.

4. Conclusion

A thermal coupling model of angular contact ball bearing with grease lubrication and fix-position preload is established based on quasi-static theory and thermal network method.

Figure 10 Comparison of experimental and calculation results

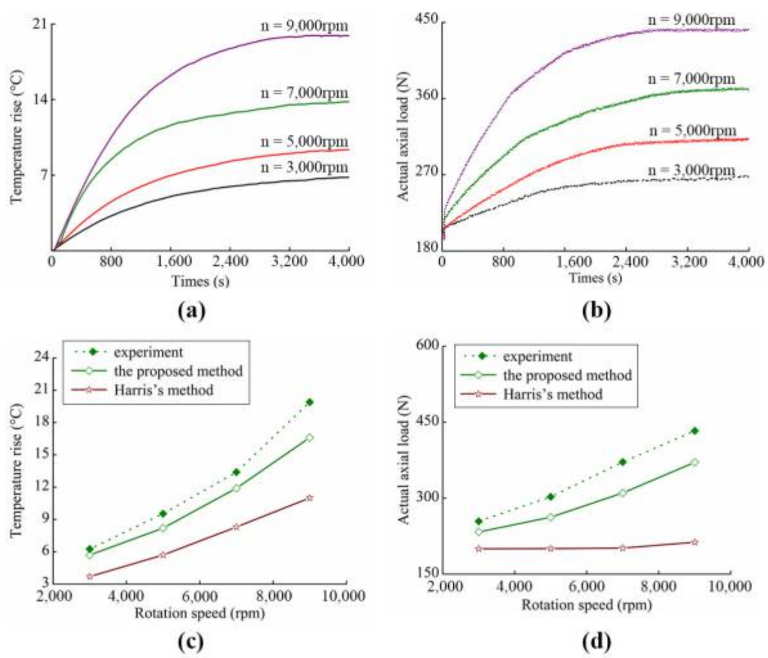

Notes: (a) Temperature rise-speed curves of outer ring; (b) actual axial load-speed curves; (c) comparison of temperature rise of outer ring; (d) comparison of actual axial load

The speed has a significant effect on bearing dynamic parameters. The higher the rotation speed, the greater the influence of thermal and centrifugal effect on the dynamic parameters of the bearing. Thermal expansion is the main factor. Under fix-position preloaded, temperature rise and the actual axial force of the bearing rise up sharply as the speed increases with thermal and centrifugal effect. Therefore, it is necessary to consider thermal and centrifugal expansion to analyze the thermo-mechanical characteristics of the bearing during the design and optimization phase of the spindle.

References

Bossmanns, B. and Tu, J.F. (1999), "A thermal model for high speed motorized spindles", *International Journal of Machine Tools and Manufacture*, Vol. 39 No. 9, pp. 1345-1366.

Bossmanns, B. and Tu, J.F. (2001), "A power flow model for high speed motorized spindles-heat generation characterization", *Journal of Manufacturing Science and Engineering*, Vol. 123 No. 3, pp. 494-505.

Cao, H.R., Zhang, X.T. and Chen, X.F. (2017), "The concept and progress of intelligent spindles: a review", *International Journal of Machine Tools and Manufacture*, Vol. 112, pp. 21-52.

Harris, T.A. (1971), "An analytical method to predict skidding in thrust loaded angular contact ball bearings", *Journal of Lubrication Technology*, Vol. 93 No. 1, pp. 17-24.

Harris, T.A. (1991), *Rolling Bearing Analysis*, 3rd ed, John Wiley & Sons, New York, NY.

Harris, T.A. and Kotzalas, M.N. (2006), "Rolling bearing analysis: advanced concept of bearing technology", 5th ed., Taylor&Francis Group, Oxford.

Holkup, T., Cao, H., Kolar, P., Altintas, Y. and Zeleny, J. (2010), "Thermo-mechanical model of spindles", *CIRP Annals-Manufacturing Technology*, Vol. 59 No. 1, pp. 365-368.

Hu, T., Yin, G.F. and Deng, C.Y. (2014), "Integrated thermo-mechanical model and analysis of angular contact ball bearing", *Journal of Sichuan University (Engineering Science Edition)*, Vol. 46 No. 4, pp. 189-198.

Hwang, Y.K. and Lee, C.M. (2010), "A review on the preload technology of the rolling bearing for the spindle of machine tools", *International Journal of Precision Engineering and Manufacturing*, Vol. 11 No. 3, pp. 491-498.

Jiang, X.Q., MA, J.J. and Zhao, L.C. (2000), "Thermal analysis of high-speed precision angular contact ball bearings", *Wear*, Vol. 8, pp. 1-4.

Jones, A.B. (1959), "Ball motion and sliding friction in ball bearing", *Journal of Basic Engineering*, Vol. 81 No. 3, pp. 1-12.

Li, H.Q. and Shin, Y.C. (2004), "Integrated dynamic thermo-mechanical modeling of high speed spindles, part 1: model development ", *Journal of Manufacturing Science and Engineering*, Vol. 126, pp. 148-156.

Lin, C.W., Tu, J.F. and Kamman, J. (2003), "An integrated thermo-mechanical-dynamic model to characterize motorized machine tool spindles during very high speed rotation", *International Journal of Machine Tools and Manufacture*, Vol. 43 No. 10, pp. 1035-1050.

Palmgren, A. (1959), *Ball And Roller Bearing Engineering*, 3rd ed., SKF industries, Burkbank, Philadelphia.

Than, V.T. and Huang, J.H. (2016), "Nonlinear thermal effects on high-speed spindle bearings subjected to preload", *Tribology International*, Vol. 96, pp. 361-372.

Tian, L.J., Hong, J., Zhu, Y.S., Li, X.H. and Guo, J.K. (2008), "Thermo-mechanical coupling model and dynamical characteristics of machining spindle-bearing system", *Journal of Xi'an Jiaotong University*, Vol. 7 No. 46, pp. 63-68.

Wang, L.Q. (2013), *Ultimate Design of Rolling Bearings*, Harbin Institute of Technology Press, Harbin.

Wang, Yl., Wang, W.Z., Zhang, S.G. and Zhao, Z.Q. (2015), "Investigation of skidding in angular contact ball bearings under high speed", *Tribology International*, Vol. 92, pp. 404-417.

Xiao, S.H., Guo, J. and Zhang, B.L. (2008), "Finite element analysis on the thermo-mechanical coupling properties of motorized spindle", *Machinery Design and Manufacture*, Vol. 9, pp. 96-98.

Yan, K., Hong, J., Zhang, J.H., Mi, W. and Wu, W.W. (2016), "Thermal-deformation coupling in thermal network for transient analysis of spindle-bearing system", *International Journal of Thermal Sciences*, Vol. 104, pp. 1-12.

Zhang, J.H., Fang, B., Hong, J. and Zhu, Y.S. (2017a), "Effect of preload on ball-raceway contact state and fatigue life of angular contact ball bearing", *Tribology International*, Vol. 114, pp. 365-372.

Zhang, J.H., Fang, B., Zhu, Y.S. and Hong, J. (2017b), "A comparative study and stiffness analysis of angular contact ball bearings under different preload mechanisms", *Mechanism and Machine Theory*, Vol. 115, pp. 1-17.

Zivkovic, A., Zeljkovic, M., Tabakovic, S. and Milojevic, Z. (2015), "Mathematical modeling and experimental testing of high-speed spindle behavior", *The International Journal of Advanced Manufacturing Technology*, Vol. 77 Nos 5/8, pp. 1071-1086.

Corresponding author

Feng Gao can be contacted at: gf2713@126.com